Available online at www.sciencedirect.com

SciVerse ScienceDirect

Physics Procedia 39 (2012) 726 – 734

Physics Procedia

LANE 2012

Pump-probe microscopy investigations on fs-laser ablation of thin Ta_2O_5/Pt layer systems

Stephan Rapp*, Janosch Rosenberger, Daniel Trappendreher, Matthias Domke, Gerhard Heise, Heinz P. Huber

Munich University of Applied Sciences, Lothstrasse 34, 80335 Munich, Germany

Abstract

A femtosecond laser is used for selective structuring of biocompatible sensorchips consisting of a Ta_2O_5/Pt layer system on glass substrate. It was observed, that for low fluences the Ta_2O_5 can be selectively lifted-off from the Pt, while high fluences enable a removal of both layers. The underlying physical effects are investigated by pump-probe microscopy allowing the observation of the whole ablation process ranging temporally from femtoseconds to microseconds. Results show the formation of a gas-liquid mixture at 3 ps, causing the Ta_2O_5 to bulge after some ns. The Ta_2O_5 is disrupted in small particles after 50 ns.

Keywords: Pump-probe microscopy, ultrashort pulse laser, thin film, biochip, ablation process

1. Motivation

In life science, biosensorchips are used especially in the field of biological screening and molecular diagnostic because of their miniaturization and the possibility to parallelize measurements [1,2]. Such a chip is shown schematically in Fig. 1 (a) and as a photograph in Fig. 1 (b).

The chip consists of an isolating tantalum pentoxide (Ta_2O_5) layer which is deposited on the conductive platinum (Pt) layer, see Fig. 2 (a). Glass acts as substrate. In contrast to the currently applied manufacturing method by different deposition and photolithographic steps, laser structuring allows a fast and uncomplicated change of the pattern and thus reduces the costs for new prototypes. In order to isolate the conducting paths, the Ta_2O_5 and the Pt has to be removed together.

* Corresponding author. Tel.: +49-89-1265-3676 ; fax: +49-89-1265-1603.
E-mail address: rapp@hm.edu.

 doi:10.1016/j.phpro.2012.10.094

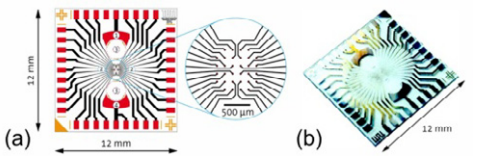

Fig. 1. (a) Layout of a biocompatible sensorchip (image by TU Munich); (b) photograph of the same sensorchip

To uncover the contacts only the Ta_2O_5 has to be ablated. These two structuring types are achieved by varying the applied laser fluence as it was shown in a recent study [3]. The schematic ablation mechanisms are displayed in Fig. 2 (a). Resulting spots are shown in Fig. 2 (b). An almost ideal blindhole is created at low fluences, see Fig. 2 (b) upper image, showing no thermal effects or damage in the Pt. At higher fluences, the Pt is ablated together with the Ta_2O_5 with a larger diameter, see Fig. 2 (b) bottom image.

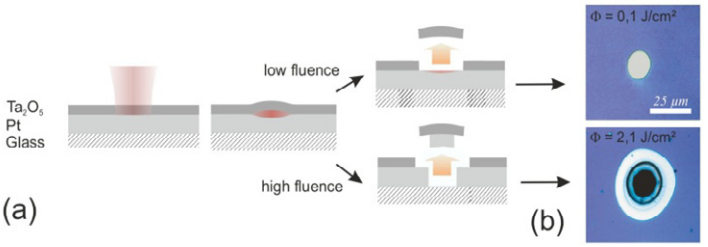

Fig. 2. (a) schematic ablation mechanism after laser irradiation from the Ta_2O_5 layer side ("indirectly-induced ablation" at low fluence); (b) light microscopy images of the final ablation state at characteristical fluences

At the applied structuring wavelength of 1053 nm, the Ta_2O_5 is transparent and the pulse energy is absorbed in the underlying Pt. The required pulse energy for the selective ablation of the Ta_2O_5 film lays below the total evaporation enthalpy of the same volume. The underlying physical effect was assumed to be a so called "indirectly-induced ablation", which was described by Heise et al. [4] investigating a comparable layer system – transparent zinc oxide (ZnO) was lifted off from absorbing copper indium diselenide (CIS). In that case, the pulse energy is absorbed in the CIS layer which is locally heated and possibly partially evaporated.The expansion of the created gas together with the thermal expansion of the ZnO layer could lead to its removal The lift-off of the transparent Ta_2O_5 on absorbing Pt corresponds to the ablation process of ZnO on CIS. Other selective removals of transparent layers from absorbing substrates by indirectly-induced laser ablation occur for example in silicon solar cell production. Here, low surface recombination losses and high backside reflectivity can be realized by passivating the silicon (Si) surface by silicon dioxide (SiO_2) or silicon nitride (SiN_x) [5,6,7]. Those transparent layers have to be opened locally for electrical contacting the solar cell.

For a deeper understanding of the underlying physical effects of indirectly-induced ablations, pump-probe microscopy is used for the temporal observation.Moreover, the removal of the Ta_2O_5 together with the Pt is investigated by pump-probe microscopy. Other groups showed in previous works, that this method is well suited to resolve ultra-fast reactions. For example pump-probe investigations with femtosecond resolution were performed on the ablation of bulk material [8,9], on the layer-side ablation of thin metal films [10,11] and on the indirectly-induced ablation of SiO_2 from Si [12]. The aim of these investigations was to measure ultrafast reflectivity changes. For this purpose, an optical delay line was

used, enabling maximal delay times of 10 to 20 ns. However, the actual lift-off takes place at later delay times. Investigations with delay times up to several microseconds were performed on silicone on titanium (Ti) [13] and on Ti or titanium nitride (TiN) on glass [14]. To cover the whole temporal range, a second electronically triggered laser was used for probing, enabling nanosecond resolution. To observe the whole ablation process with sub-picosecond resolution in the first 4 ns and sub-nanosecond resolution at higher delay times, we combined both probing methods for the first time to our knowledge [15,16].

Here, the structuring of a 200 nm Ta_2O_5/400 nm Pt/glass sample is investigated at two different fluences Φ (pulse energy per area). At a fluence of $\Phi = 0.1$ J/cm² the Ta_2O_5 is selectively ablated and at $\Phi = 2.1$ J/cm² the Pt is removed as well.

2. Material and methods

For the experiments 3" glass wafers (0.5 mm) were used as substrate. Platinum films of 400 nm thickness were deposited by RF sputtering. The Ta_2O_5 layer of 200 nm thickness was deposited by ion-assisted electron-beam evaporation.

A short overview of the setup is sketched in Fig. 3. A laser pulse at a center wavelength of $\lambda = 1053$ nm (pulse length $\tau = 660$ fs FWHM) is divided into pump and probe pulse by beam splitter 1. The pump pulse, used for initiating the ablation, is focused on the sample, whereas the probe pulse is frequency doubled (SHG) and optically delayed by a linear translation stage up to delay times of $\Delta t = 4$ ns. For probing with delay times above 4 ns, a 600 ps FWHM laser source emits a second probe pulse ($\lambda = 532$ nm). Both probe pulses are combined in beam splitter 2 for coaxial illumination of the sample. Then, the ultrafast exposed sample is imaged by a microscope and a CCD camera (calculated optical resolution $R = \lambda/\text{numerical aperture} = 1.22$ µm). A detailed description of the pump-probe microscopy setup is given in an earlier paper [15], also showing calibration of the temporal zero point and image acquiring and processing.

Thus, the whole time frame of the ablation process ranging from femtoseconds to microseconds can be covered with both probe sources, achieving a temporal resolution (= cross correlation time) of 840 fs during the first 4 ns and a 800 ps resolution for later delay times. The reaction onset is always initiated by the ultra-fast pump pulse. Reflectivity changes higher than 2% can be detected.

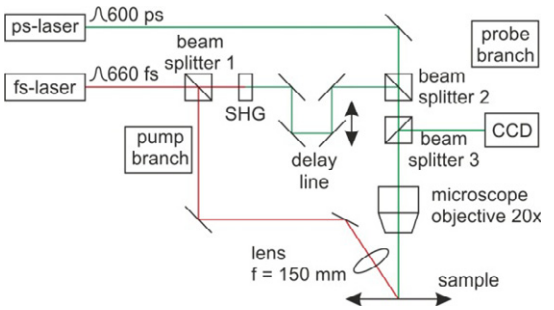

Fig. 3. Pump-probe microscopy setup: A 660 fs laser pulse is split in two parts (beam splitter 1). The first part (red pump branch) is focused at the sample and initiates the reaction. The second part (green probe branch) is frequency doubled (SHG) and temporally delayed for illumination (delay line for $\Delta t < 4$ ns). For $\Delta t > 4$ ns a 600 ps laser pulse is emitted by a second laser. A picture is captured by a CCD camera

3. Results

3.1. Ablation threshold determination

The single pulse ablation thresholds Φ_{thr} for the selective removal of Ta_2O_5 (200 nm Ta_2O_5 on 400 nm Pt) and the removal of both layers (200 nm Ta_2O_5 with 400 nm Pt) are determined with a method described by Liu [17]. The area of the ablated spot increases linearly with the logarithm of the applied fluence, see Fig. 4. The good agreement of linear fit function and data points indicates an almost ideal threshold behavior for both reaction types over more than two respectively one order of magnitude in fluence. The threshold fluence level of the corresponding process is defined when the extrapolated graph reaches an area of zero. The threshold fluences were determined to be Φ_{thr} = 0.06 J/cm² (200 nm Ta_2O_5 on 400 nm Pt) and Φ_{thr} = 1.21 J/cm² (200 nm Ta_2O_5 with 400 nm Pt) (accuracy = ±5 %). To investigate the two ablation types, two fluences were chosen for time resolved measurements (Φ = 0.1 J/cm² and Φ = 2.1 J/cm²) that lay right above those threshold fluences.

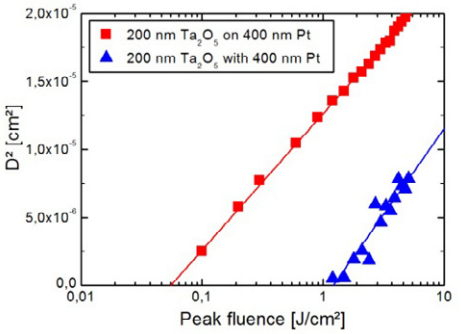

Fig. 4. Ablation threshold determination of a 200 nm Ta_2O_5 / 400 nm Pt layer stack. The squared ablation diameters D² are plotted against the applied fluence. The threshold fluence level Φ_{thr} of the corresponding process is defined when the extrapolated graph reaches an area of zero. Φ_{thr} = 0.06 J/cm² (200 nm Ta_2O_5 on 400 nm Pt) and Φ_{thr} = 1.21 J/cm² (200 nm Ta_2O_5 with 400 nm Pt)

3.2. Pump-probe microscopy investigation

Pump-probe images of the ablation processes at significant delay times indicated in the top left corners are shown in Fig. 5. The applied fluence Φ is varied between the upper two rows (Φ = 0.1 J/cm²) and the lower two rows (Φ = 2.1 J/cm²). The pump pulse hits the sample from the layer side as it was shown in Fig. 2 (a). The pictures are taken from the same side.

3.2.1. Irradiation with low fluence (Φ = 0.1 J/cm²) – indirectly-induced ablation

Around delay time zero the pump pulse irradiates the sample (Δt = 0 s). After 1 ps no significant changes can be observed. At 3 ps, a dark area appears at the irradiated spot. The relative reflectivity decrease in the center of this spot is determined to be about -20%, see Fig. 6. The reflectivity remains on that level up to a delay time of 30 ps. However, the diameter of the dark spot decreases slightly between 3 ps and 30 ps. At 125 ps the irradiated area becomes brighter ($\Delta R/R$ = +30%, see Fig. 6). At 1 ns and 2 ns the relative reflectivity continues to increase ($\Delta R/R$ = +170% at 1 ns, see Fig. 6). The shape of this bright spot has very well defined edges compared to the dark spot at earlier delay times, see black dotted lines.

At delay times of 10 ns and 20 ns ring systems are formed in the bright spot center and in the surrounding area that will be discussed in the next section. At 50 ns and 100 ns cracks are created in the spot center and after 1 µs flying particles can be observed that leave the focus plane. They disintegrate from the sample and fly in direction of the CCD camera. The final state the Pt is uncovered and a clean hole free from thermal effects is created in the Ta_2O_5 layer.

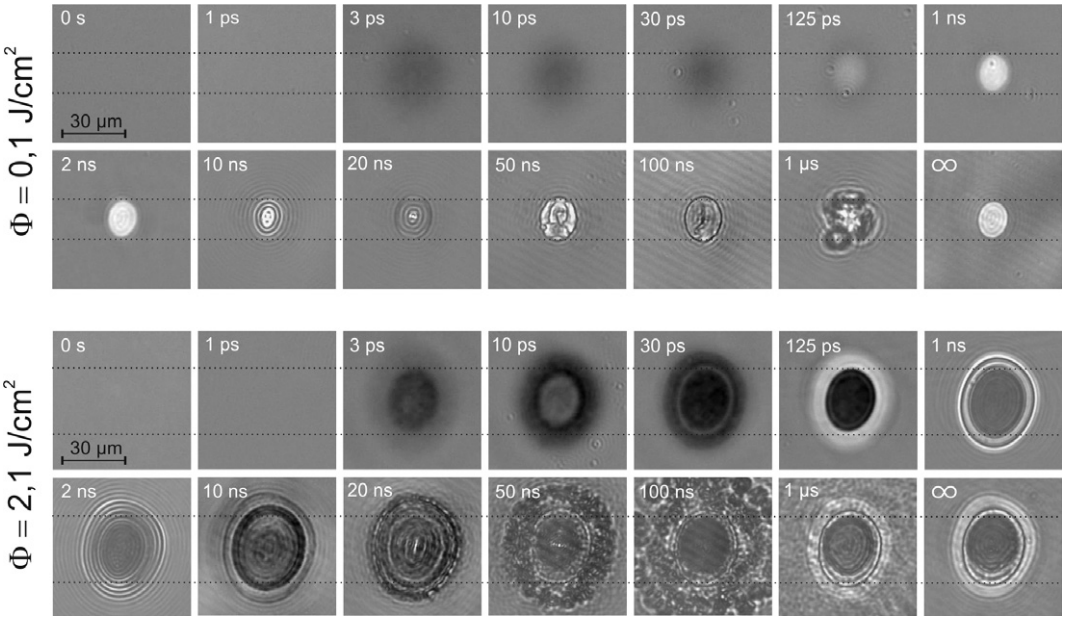

Fig. 5. Pump-probe images at different significant delay times indicated in the left upper corners of the pictures of a 200 nm thick Ta_2O_5 layer on 400 nm Pt ablated with a 1053 nm/660 fs pulse at two different fluences of Φ = 0.1 J/cm² (upper two rows) and Φ = 2.1 J/cm² (lower two rows)

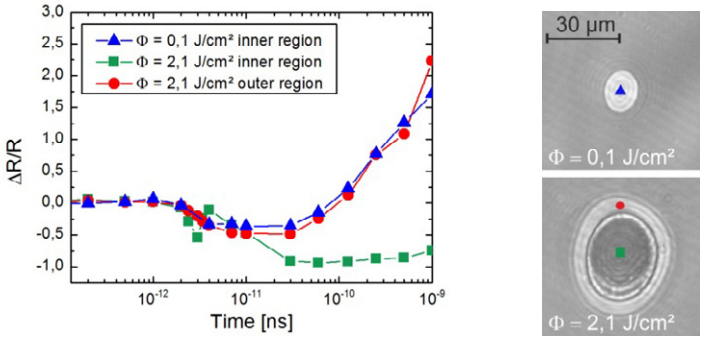

Fig. 6. Relative reflectivity change ΔR/R over the time at the irradiation of a 200 nm thick Ta_2O_5 layer on 400 nm Pt with a 1053 nm/660 fs pulse at two different fluences of Φ = 0.1 J/cm² and Φ = 2.1 J/cm², see left figure. The relative reflectivity is determined in the spot center, see right figure blue triangle and green square, and at the outer region, see right figure red dot; $\Delta R/R = (R_{during}-R)/R$; with R_{during} ≙ reflectivity at the investigated delay time and R ≙ reflectivity before the irradiation

3.2.2. Irradiation with high fluence (Φ = 2.1 J/cm²)

Similar to the measured series at a fluence of Φ = 0.1 J/cm², the pump-probe images - taken at a fluence of Φ = 2.1 J/cm² - show no visible reactions at delay times of 0 s and 1 ps. At 3 ps first changes in the material can be observed. In contrast to the measurements at the lower fluence where a homogeneous dark spot is created, the pictures taken at a fluence of Φ = 2.1 J/cm² show two areas with different transient behavior at delay times later than 3 ps. The areas are separated by the black dotted lines in Fig.5. The inner region is indicated by a green square (center) and the outer region by a red dot (border) (Fig. 6).

At 3 ps a dark spot is created in the inner region surrounded by a less dark area in the outer region. For delay times of up to 1 ns, the relative reflectivity in the outer region shows an identical transient behavior as the reflectivity in the spot center for a fluence of Φ = 0.1 J/cm², see Fig. 6 red dots and blue triangles. Assuming a Gaussian beam profile, the fluence in that outer region was calculated to be about Φ = 0.3 J/cm².

In the spot center, the reflectivity decreases faster than in the outer region. The first minimum at ΔR/R = -60% is reached at about 3 ps, see Fig. 6. At 10 ps the spot center becomes slightly brighter again (ΔR/R = -40%) and after 30 ps the second reflectivity minimum is reached at a level of about ΔR/R = -90%. Up to the delay time of 1 ns the relative reflectivity in the spot center remains on that level.

At 2 ns, ring systems are created in the outer region that are comparable to those observed at the lower fluence at 10 ns. The inner region remains dark. Between 10 ns and 50 ns small particles are disintegrating in the outer region, while in the inner region no particles are visible (Fig. 6). Moreover a radial shock wave with an average velocity of about 900 m/s can be observed at delay times later 10 ns, see Fig. 7. At 100 ns and 1 µs the particles are flying in direction of the camera leaving the field of depth. In the final state, a dark area in the inner region, where the Pt is ablated, is surrounded by a brighter ring in the outer region, where only the Ta_2O_5 is removed.

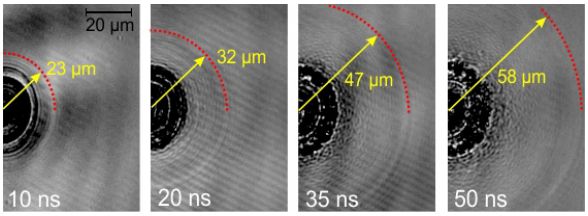

Fig. 7. Shock wave propagation in air after irradiation of a 200 nm thick Ta_2O_5 layer on 400 nm Pt with a 1053 nm/660 fs pulse at a fluence of Φ = 2.1 J/cm². The delay times are indicated in the corner bottom left. The contrast of the pictures is enhanced to improve the visibility of the shock wave. The red dotted line marks the wave front. The yellow arrow shows the wave radius

4. Discussion

First, the temporal behavior of the Ta_2O_5 lift-off from the Pt is regarded. This effect, called indirectly-induced ablation, occurs for a fluence of 0.1 J/cm², as well as in the outer region at 2.1 J/cm². The laser pulse irradiates the sample at delay time zero. The ablation process can be explained in the following way: the pump pulse is transmitted through the Ta_2O_5 and its energy is absorbed by free electrons in the Pt. The electrons in the Pt then transfer their energy to the lattice, causing ultrafast melting [18,19]. The reflectivity changes during the first picoseconds are too low to be detected here. At 3 ps, a reflectivity decrease is observed, which is probably caused by probe light scattering in a homogeneous gas-liquid

mixture, which results from a confined phase explosion [16]. The confinement of the homogeneous gas-liquid mixture causes high pressure and temperature at the Pt/Ta_2O_5 interface probably leading to a shock wave in both layers. At about 125 ps, the shock wave, the expansion of the gas-liquid mixture and possibly the thermal expansion of the Ta_2O_5 film initiate the delamination of the Ta_2O_5 film. The volume at the layer interface then expands and the gas-liquid mixture recondenses due to adiabatic cooling. This scenario would explain the increased reflectivity at 1 ns. The ring systems, created at 10 ns (Φ = 0.1 J/cm²) in the spot center or at 2 ns (Φ = 2.1 J/cm²) in the outer region, correspond to Newton's rings – which originate from interference of light reflections from the Ta_2O_5 dome and the flat Pt surface. The Ta_2O_5 film continues to bulge until the tensile stress limit is reached. Then, the Ta_2O_5 disintegrates in small particles, observed at about 20 to 50 ns. As a result, the Pt is completely uncovered without thermal damages at 0.1 J/cm², as well as in the outer region at 2.1 J/cm².

Now, the removal of Pt and Ta_2O_5 in the inner region at a fluence of 2.1 J/cm² is considered. At 3 ps, a steep reflectivity increase can be observed at the transition from the inner region ($\Delta R/R$ = -60%) to the outer region ($\Delta R/R$ = -20%). Generally the lower relative reflectivity in the center region shows a progressing phase explosion of the film system, resulting in a complete removal of Pt and Ta_2O_5 film. Further investigations of the irradiation of a Ta_2O_5 layer on glass without intermediate Pt film are needed to understand the oscillating reflectivity trend in the delay time range between 3 ps and 1 ns. At delay times between 10 ns and 100 ns, the disintegration of the Ta_2O_5 can be observed in the outer region. However, the removal of the Ta_2O_5 and the Pt in the center cannot be observed as clearly as in the outer region. Hence, both layers could either be completely evaporated, or the size of the ejected particles is too small to be resolved by the microscope.

At about 10 ns, an expanding ring can be observed in Fig. 7. The ring can be identified as shock wave propagation in air, as seen by other pump–probe observations from the side [10]. The shock wave front can be observed before the outer region disintegrates. It could be initiated either by ultrafast expansion of the completely evaporated inner region, or by a shockwave that was generated by the confined phase explosion in the Ta_2O_5 and transferred to air. The shock wave may reduce the energy needed for a removal of the Pt and Ta_2O_5 film. We think that the irradiating energy is only slightly exceeding the evaporation enthalpy of Pt and Ta_2O_5. Comparing the energy efficiency with the direct laser ablation of an uncovered 400 nm Pt film at a threshold fluence of 5.3 J/cm² [21], we conclude that the shock wave is lowering the needed energy making the laser removal more efficient.

5. Conclusion

In this paper a pump-probe microscope is used that combines an optical and an electronic delay for the complete observation of laser ablation processes ranging temporally from picoseconds to microseconds. It was shown that the irradiation of a Ta_2O_5/Pt layer stack allows the selective removal of the Ta_2O_5 at a low fluence of Φ = 0.1 J/cm², caused by an indirectly-induced ablation, and enables the ablation of both layers at a higher fluence of Φ = 2.1 J/cm².

For the lower fluence the reaction initiation – the pulse absorption by free electrons in the Pt (0 s) - is followed by energy transfer to the Pt lattice, subsequent ultrafast melting and the creation of a gas-liquid-mixture at the surface of the layer (3 ps). The inertial confinement by the transparent Ta_2O_5 causes a steep rise of pressure and temperature, both creating an energy transfer from the interface layer to the transparent film. At around 125 ps the transparent film delaminates and the evaporated material of the absorbing layer condenses. At around 1 ns the film starts to bulge and at about 20 ns the maximum height is reached. Then, the Ta_2O_5 layer disintegrates (50 ns). In the final state, an almost ideal blind hole without thermal damages is created in the transparent film uncovering the underlying Pt layer.

The irradiation with the higher fluence shows a different behavior – two different areas can be distinguished: the area in the spot center with a diameter of about 20 µm and the surrounding area (outer region) where the fluence was calculated to be about $\Phi = 0.3$ J/cm². Here, an analogical reaction process compared to the first series of measurement with a fluence of $\Phi = 0.1$ J/cm² is observed. In the spot center, where the Pt is ablated as well, the process cannot be observed as clearly as in the outer region. Here, the high fluence might have caused a complete evaporation of both layers, initiating a visible shock wave in air. Further investigations have to be undertaken to completely understand these effects.

For the described ablation types, process speeds over 20 m/s for the selective removal of Ta_2O_5 respectively more than 1 m/s for the ablation of the Ta_2O_5/Pt layer stack can be reached for 1 W of irradiated laser power. Hence, ultrafast lasers can provide precise and selective processes at extremely high efficiencies for maskless patterning and production.

Acknowledgements

This work was partly funded by the German Federal Ministry of Education and Research within the project “METASOLAR” under the grant No. 02PO2851. We thank Christiane Fritze and Jürgen Meier for financial support by the Munich University of Applied Science, and Michael Kaiser for technical support.

References

[1] Gross, G.W.; Rieske, E.; Kreutzberg, G.W.; Meyer, A.: A new fixed-array multi-microelectrode system designed for long-term monitoring of extracellular single unit neuronal activity in vitro. *Neurosc. Lett.* 1977; **6**: pp. 101–105.

[2] Johnstone, A.; Gross, G.W.; Weiss, D.G.; Schroeder, O.; Gramowski, A.; Shafer, T.:W.; White, E.B.: Microelectrode arrays: A physiologically based neurotoxicity testing platform for the 21st century. *NeuroToxicology*. 2010, **31**: 331-350.

[3] Heise, G.; Trappendreher, D.; Ilchmann, F.; Weiss, R.S.; Wolf, B.; Huber, H.P.: Picosecond laser structuring of thin film platinum layers covered with tantalum pentoxide isolation. *J. Appl. Phys.* 2012, **112**: 013110.

[4] Heise, G.; Dickmann, M.; Domke, M.; Heiss, A.; Kuznicki, T.; Palm, J.; Richter, I.; Vogt, H.; Huber, H. P.: Investigation of the ablation of zinc oxide thin films on copper-indium-selenide layers by ps laser pulses. *Appl. Phys. A* 2011, **104**: pp. 387-393.

[5] Hermann, S.; Neubert, T.; Wolpensinger, B.; Harder, N.-P.; Brendel, R.: Proces characterization of picosecond laser ablation of SiO2 and SiNx layers on planar and textured surfaces. 23rd European Photovoltaic Solar Energy Conference, Valencia, Spain 2008.

[6] Blakers, A.W.; Wang, A.; Milne, A.M.; Zhao, J.; Green, M.A.: 22,8% efficient silicon solar cell. *Appl. Phys. Lett*. 1989, **55**: 1363-1365.

[7] Rana, V.V.; Zhang, Z.: Selective removal of dielectric layers using picosecond UV pulses. *Proc. of SPIE* 2009, **7193**.

[8] Von der Linde, D.; Sokolovski-Tinten, K.: The physical mechanism of short-pulse laser ablation . *Appl. Surf. Sci.* 2000; **154**: pp. 1–10.

[9] Bonse, J.; Bachelier, G.; Siegel, J.; Solis, J.; Sturm, H.: Time- and space-resolved dynamics of ablation and optical breakdown induced by femtosecond laser pulses in indium phosphide. *J. Appl. Phys.* 2008, **103**: 054910.

[10] Mingareev, I.; Horn, A.: Melt dynamics of aluminium irradiated with ultrafast laser radiation at large intensities. *J. Appl. Phys.* 2009, **106**: 013513.

[11] Von der Linde, D.; Sokolovski-Tinten, K.; Bialkowski, J.: Laser-solid interaction in the femtosecond time regime. *Appl. Surf. Sci* 1997, **109-110**: pp. 1-10.

[12] McDonald, J.P.; Nees, J.A.; Yalisove, S.M.: Pump-probe imaging of femtosecond pulsed laser ablation of silicon with thermally grown oxide films. *J. Appl. Phys.* 2007, **102**: 063109.

[13] Dlott, D.D.: Ultra-low threshold laser ablation investigated by time-resolved microscopy. *Appl. Surf. Sci.* 2002; **197-198**: pp. 3–10.

[14] Koulikov, S.G.; Dlott, D.D.: Ultrafast microscopy of laser ablation of refractory materials: ultra low threshold stress-induced ablation. *J. Photochem. Photobiol. A: Chem.* 2001, **145**: pp. 183-194.

[15] Domke, M.; Rapp, S.; Schmidt, M.; Huber, H.P.: Ultrafast pump-probe microscopy with high temporal dynamic range. *Opt. Expr.* 2012, **20**: pp. 10330-10338.

[16] Domke, M.; Rapp, S.; Schmidt, M.; Huber, H.P.: Ultrafast movies of thin film laser ablation. *Appl. Phys. A* 2012, **10.1007**.

[17] Liu, J.M.: Simple technique for measurements of pulsed Gaussian-beam spot sizes. *Opt. Lett. A* 1982, **7**: pp. 196-198.

[18] Rethfeld, B.; Sokolovski-Tinten, K.; Von der Linde, D.; Anisimov, S.I.: Timescales in the response of materials to femtosecond laser excitation. *Appl. Phys. A* 2004, **79**: pp. 767-769.

[19] Sundaram, S.K.; Mazur, E.: Inducing and probing non-thermal transitions in semiconductors using femtosecond laser pulses. *Nat. Mater.* 2002, **1**: pp. 217-224.

[20] Mingareev, I.; Horn, A.: Time-resolved investigations of plasma and melt ejections in metals by pump-probe shadowgraphy. *Appl. Phys. A.* 2008, **92**: pp. 917-920.

[21] G. Heise, G.; Trappendreher, D.; Ilchmann, F.; Weiss, R.S.; Wolf, B.; Huber, H.P.: Picosecond laser structuring of thin film platinum layers covered with tantalum pentoxide isolation. *J. Appl. Phys.* 2012, **112**: pp. 013110-6.